HAL
open science

AAV9-Mediated Expression of SMN Restricted to Neurons Does Not Rescue the Spinal Muscular Atrophy Phenotype in Mice

Aurore Besse, Stephanie Astord, Thibaut Marais, Marianne Roda, Benoit Giroux, François-Xavier Lejeune, Frederic Relaix, Piera Smeriglio, Martine Barkats, Maria Grazia Biferi

To cite this version:

Aurore Besse, Stephanie Astord, Thibaut Marais, Marianne Roda, Benoit Giroux, et al.. AAV9-Mediated Expression of SMN Restricted to Neurons Does Not Rescue the Spinal Muscular Atrophy Phenotype in Mice. Molecular Therapy, 2020, 28 (8), pp.1887-1901. 10.1016/j.ymthe.2020.05.011 . inserm-03130706

HAL Id: inserm-03130706

https://inserm.hal.science/inserm-03130706

Submitted on 3 Feb 2021

HAL is a multi-disciplinary open access archive for the deposit and dissemination of scientific research documents, whether they are published or not. The documents may come from teaching and research institutions in France or abroad, or from public or private research centers.

L'archive ouverte pluridisciplinaire **HAL**, est destinée au dépôt et à la diffusion de documents scientifiques de niveau recherche, publiés ou non, émanant des établissements d'enseignement et de recherche français ou étrangers, des laboratoires publics ou privés.

Molecular Therapy
Original Article

AAV9-Mediated Expression of SMN Restricted to Neurons Does Not Rescue the Spinal Muscular Atrophy Phenotype in Mice

Aurore Besse,[1] Stephanie Astord,[1] Thibaut Marais,[1] Marianne Roda,[1] Benoit Giroux,[1] François-Xavier Lejeune,[2] Frederic Relaix,[3] Piera Smeriglio,[1] Martine Barkats,[1,4] and Maria Grazia Biferi[1,4]

[1]Sorbonne Université, INSERM, Institute of Myology, Centre of Research in Myology, 75013 Paris, France; [2]Institut du Cerveau et de la Moelle épinière (ICM), Bioinformatics and Biostatistics Core Facility (iCONICS), Sorbonne Université, INSERM U1127, CNRS UMR 7225, GH Pitié-Salpêtrière, 75013 Paris, France; [3]Université Paris Est Créteil, INSERM, EnvA, AP-HP, 94000 Créteil, France

Spinal muscular atrophy (SMA) is a neuromuscular disease mainly caused by mutations or deletions in the *survival of motor neuron 1* (*SMN1*) gene and characterized by the degeneration of motor neurons and progressive muscle weakness. A viable therapeutic approach for SMA patients is a gene replacement strategy that restores functional SMN expression using adeno-associated virus serotype 9 (AAV9) vectors. Currently, systemic or intra-cerebrospinal fluid (CSF) delivery of AAV9-SMN is being explored in clinical trials. In this study, we show that the postnatal delivery of an AAV9 that expresses SMN under the control of the neuron-specific promoter synapsin selectively targets neurons without inducing re-expression in the peripheral organs of SMA mice. However, this approach is less efficient in restoring the survival and neuromuscular functions of SMA mice than the systemic or intra-CSF delivery of an AAV9 in which SMN is placed under the control of a ubiquitous promoter. This study suggests that further efforts are needed to understand the extent to which SMN is required in neurons and peripheral organs for a successful therapeutic effect.

INTRODUCTION

Spinal muscular atrophy (SMA) is a neuromuscular disorder considered to be one of the leading genetic causes of infant death in children younger than 2 years of age.[1–3] SMA is characterized by progressive degeneration of the lower motor neurons (MNs) and muscle weakness, leading to paralysis and premature death in the most severe cases.[4,5] In 95% of cases, SMA is caused by homozygous deletions or mutations in the telomeric copy of the *survival of motor neuron 1* (*SMN1*) gene, inducing loss of the SMN protein.[6] The presence of the *SMN2* gene, an almost identical gene, can act as a disease modifier in humans. Although *SMN2* mostly leads to the production of an unstable truncated form of SMN (lacking exon 7 and called SMNΔ7), residual levels of full-length SMN protein (5%–10%) are nevertheless produced, but they are insufficient to fully compensate for the loss of *SMN1*.[6]

Together with the approved antisense oligonucleotide therapy nusinersen (Spinraza),[7,8] the US Food and Drug Administration (FDA) has approved a therapeutic approach based on the stable replacement of *SMN1* using viral vectors, called onasemnogene abeparvovec (Zolgensma).[9,10]

We and others have contributed to a significant breakthrough in this domain, discovering the efficiency of self-complementary adeno-associated viral vector of serotype 9 (AAV9) for central nervous system (CNS) gene transfer upon systemic injection.[11–13] We have used this method to demonstrate that intravenous (i.v.) delivery of SMN through AAV9 vectors can rescue a severe animal model of SMA.[14] These mice, with a mean lifespan of 14 days, are knocked out for the endogenous *Smn* gene and express the human *SMN2* gene together with the truncated SMN cDNA (SMNΔ7 mice).[15] SMNΔ7 mice survive for an average of 160 days[14] when treated via i.v. injection with an AAV9 carrying an optimized *SMN1* cDNA under the control of a ubiquitous promoter. Other groups have independently reported similar results,[16,17] and the AAV9-based treatment originally developed by Foust et al.[16] received FDA approval for SMA type I patients. Among treated children, the best results in terms of motor function recovery were found in the cohort injected with the highest amount of SMN-expressing AAV9.[10] However, the long-term effects of systemic delivery of such a high dose of AAV vector are still unknown and could be detrimental. Indeed, elevated aminotransferase levels, an indicator of liver damage, were observed in some AAV9-SMN-treated patients.[10] This, together with severe toxicity, has also been observed in non-human primates (NHPs) and piglets after i.v. injection of an AAV9-SMN vector with a modified capsid (AAVhu68).[18] Therefore, reducing the viral load while maintaining efficient targeting of the CNS and MNs is crucial for improving an effective and safe SMN gene replacement therapy.

Received 12 March 2020; accepted 12 May 2020;
https://doi.org/10.1016/j.ymthe.2020.05.011.

[4]Senior author

Correspondence: Maria Grazia Biferi, Sorbonne Université, INSERM, Institute of Myology, Centre of Research in Myology, 75013 Paris, France.
E-mail: mg.biferi@institut-myologie.org

This is an open access article under the CC BY-NC-ND license (http://creativecommons.org/licenses/by-nc-nd/4.0/).

Advances in this direction have been achieved in animal studies through the evaluation of alternative delivery routes for AAV9-SMN. Indeed, vector administration via intramuscular[19] or intracerebrospinal fluid (CSF) injections[20–24] at lower doses than those used for systemic delivery in SMA type I patients[10] successfully promoted a rapid and long-lasting correction of SMN levels and phenotypic rescue in SMNΔ7 mice. Effective CNS transduction after intra-CSF delivery of AAV9 vectors has been successfully demonstrated in larger animals and NHPs as well.[22,23,25–29] Currently, the efficacy, safety, and tolerability of direct delivery of AAV9-SMN into the CSF are being evaluated in an ongoing clinical trial for SMA type II patients (ClinicalTrials.gov: NCT03381729). However, the FDA placed a partial hold on this study for enrollment in the high-dose cohort. This was based on unpublished pre-clinical data reporting inflammation and neural degeneration in the dorsal root ganglia of injected animals (https://www.novartis.com/news/media-releases/novartis-announces-avxs-101-intrathecal-study-update). If confirmed, these data suggest that added care must be taken to determine the proper vector dosing in the CSF of patients.

The most efficient AAV-mediated gene replacement therapies developed to date for SMA utilize ubiquitous promoters to control SMN expression.[10,14,16,22] Although these approaches have rescued the SMA phenotype, it is still debated whether the beneficial effects are exclusively due to CNS-specific rescue or to the synergistic effects of the therapy on MNs and other cell types.[30–32] Indeed, SMA is traditionally considered to be a specific MN disease, but in the last few years, several studies have demonstrated that other organs, such as skeletal muscle[33–35] and neuromuscular junctions,[36–39] liver,[40–42] heart,[43–45] pancreas,[46,47] and vascular[48] or immune systems[49] are also affected. Further research is thus needed to elucidate the degree of the peripheral contribution and the level of SMN restoration required in the CNS to induce the most desirable rescue of the SMA phenotype.[50]

We sought to address the question of the tissue requirement for SMN by exploring the effects of neuron-selective SMN replacement on the severe SMA phenotype relative to those of ubiquitous targeting.

We generated a novel AAV9 vector expressing SMN under the control of the human synapsin (SYN) promoter (AAV9-SYN-SMN) and studied the effects of AAV9-SYN-SMN delivery on the survival and neuromuscular functions of SMNΔ7 mice. We then compared this treatment to AAV9-mediated delivery of SMN controlled by the ubiquitous phosphoglycerate kinase (PGK) promoter (AAV9-PGK-SMN). We administered AAV9-PGK-SMN via i.v. or intracerebroventricular (i.c.v.) injection, providing the first direct comparison of these two clinically relevant delivery routes.

Our data not only show that restoring SMN production in neurons, including MNs, only partially rescues SMNΔ7 mice, but they also show the importance of SMN re-expression in peripheral organs, such as skeletal muscle, heart, and liver. Mice systemically treated with AAV9-PGK-SMN survived substantially longer than animals treated with AAV9-SYN-SMN, although SMN levels in the CNS tissues and MN transduction were similar. We also report that the i.c.v. injection of AAV9-PGK-SMN outperforms systemic administration of the same vector, providing supraphysiological levels of SMN in the CNS organs and re-establishing SMN expression in the periphery.

This study demonstrates the importance of appropriate peripheral targeting and suggests that optimal levels of SMN in each tissue should be defined to ensure a therapeutic effect of gene replacement strategies and, more generally, SMN-targeted approaches for SMA treatment.

RESULTS

i.c.v. Injection of AAV9-SYN-SMN at a High Dose Efficiently Transduces the Spinal Cord of SMNΔ7 Mice but Not Peripheral Organs

Our objective was to investigate whether the neuron-targeted expression of SMN is sufficient to rescue the SMNΔ7 mouse phenotype as well as the broadly used ubiquitous promoters.[14,16,17,20] We thus used the human SYN promoter, which has previously been shown effective in targeting expression in neuronal cells with AAV vectors.[51–53] We produced an AAV vector encoding an optimized *SMN1* cDNA under the control of the human neuronal promoter SYN (AAV9-SYN-SMN) (Figure 1A). We ensured selective transduction of AAV9-SYN-SMN into neurons by directly administering the vector into the lateral ventricles of SMNΔ7 mice through a single-dose i.c.v. injection (Figure 1A).

We first evaluated SMN expression levels after i.c.v. injection at postnatal day 1 (PND1) of the newly generated AAV9-SYN-SMN vector in the spinal cords of SMNΔ7 mice by western blotting.[54] We tested two different doses: 4.5×10^{10} viral genomes (vg)/mouse (low) and an ~3-fold higher dose, 1.2×10^{11} vg/mouse (high).

Injection of AAV9-SYN-SMN at the low dose was not sufficient to induce a significant increase in SMN expression over that observed in untreated SMNΔ7 mice, confirming the reported weakness of the SYN promoter[52] (Figure 1B). On the contrary, the higher dose of AAV9-SYN-SMN induced significant rescue of SMN protein expression in the spinal cords of SMNΔ7 mice (Figure 1B). The variability of SMN expression levels observed in mice treated with the low dose of SMN was higher than that in mice injected with the high dose, likely contributing to the inefficiency of SMN re-expression.

We also assessed the specificity of the SYN promoter by analyzing SMN expression outside the CNS. SMN protein was barely detected in the skeletal muscle, heart, or liver of SMNΔ7 mice injected with AAV9-SYN-SMN (high) (Figure 1C). The expression was similar to that of non-injected SMNΔ7 mice, showing selectivity of the SYN promoter (Figure 1C).

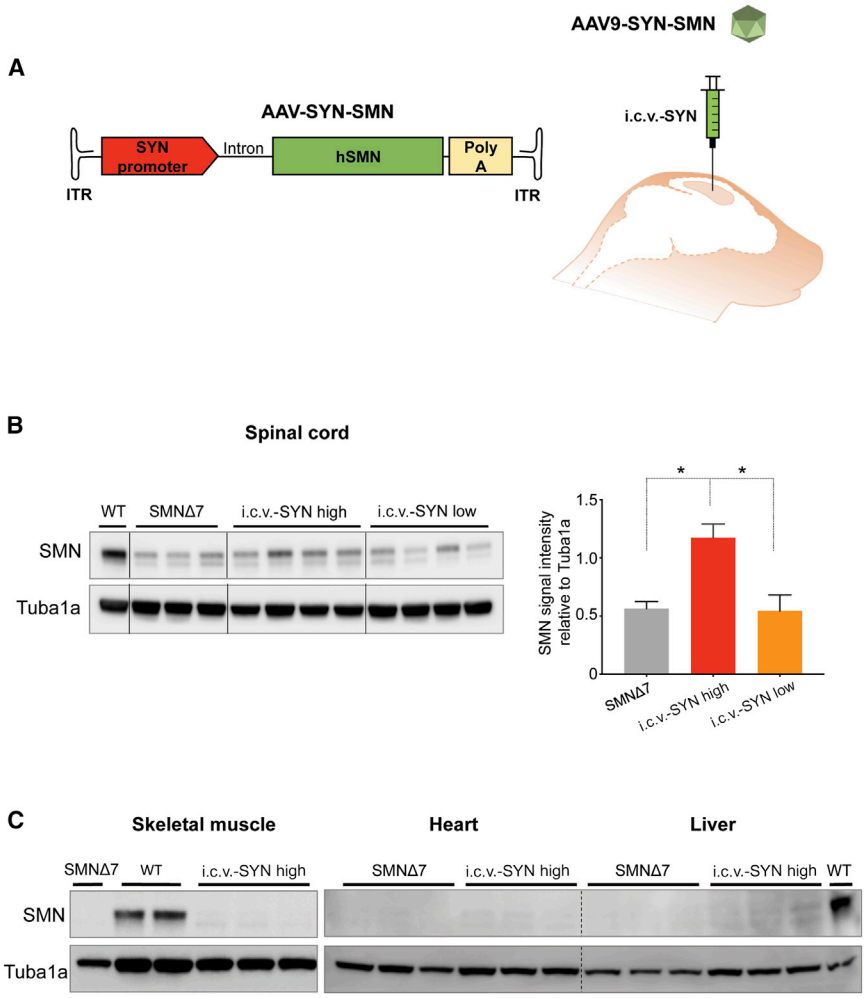

Figure 1. i.c.v. Injection of the High Dose of AAV9-SYN-SMN Transduces the Spinal Cords of SMNΔ7 Mice, but Not Peripheral Organs

(A) Schematic representation of the AAV construct expressing SMN under the control of the neuron-specific human synapsin promoter (AAV9-SYN-SMN) (left) and schematic representation of its delivery into the lateral ventricles of SMNΔ7 mice (intracerebroventricular [i.c.v.] injection) (right). The optimized sequence of human *SMN1* (hSMN) cDNA (green box) is expressed under control of the SYN promoter (red box). The chimeric intron (Intron) is placed between the promoter and the SMN cDNA and the polyadenylation (poly(A) signal of SV40 (yellow box) downstream of the SMN cDNA. The entire cassette is inserted between the two self-complementary inverted terminal repeats (ITRs) of an AAV2 genome. (B) Left: western blot analyses of SMN expression (37 kDa) in the spinal cords of 14-day-old SMNΔ7 mice after i.c.v. injection of AAV9-SYN-SMN at 1.2×10^{11} vg/mouse (i.c.v.-SYN-SMN high, number of animals, n = 4) and 4.5×10^{10} vg/mouse (i.c.v.-SYN-SMN low, n = 4). Protein lysates from age-matched wild-type (WT) mice (n = 1) and untreated SMNΔ7 mice (n = 3) were used as the reference for SMN expression. α-Tubulin (Tuba1a, 50 kDa) was used as the loading control. Right: densitometric analysis of the western blot signal in the spinal cords of injected SMNΔ7 mice. Statistical analysis was performed on SMNΔ7 (n = 3), i.c.v.-SYN high (n = 4), and i.c.v.-SYN low (n = 4) mice. There was no statistical difference in SMN expression between untreated SMNΔ7 mice and those injected i.c.v. with AAV9-SYN-SMN, whereas i.c.v. injection of the high dose of AAV9-SYN-SMN resulted in a significant increase of SMN expression. Values are expressed as the SMN mean signal intensity relative to that of Tuba1a ± SEM, and the differences between groups were analyzed by one-way ANOVA followed by Tukey's *post hoc* test (*$p < 0.05$). (C) Western blot analyses of SMN expression (37 kDa) in skeletal muscle, heart, and liver of 14-day-old SMNΔ7 mice injected i.c.v. with AAV9-SYN-SMN at a dose of 1.2×10^{11} vg/mouse (i.c.v.-SYN high), showing a weak SMN signal. Age-matched non-injected SMNΔ7 mice (n = 1 for muscle and n = 3 for heart and liver) and WT mice (n = 2 for muscle and n = 1 for liver) were used as references for SMN expression. Tuba1a (50 kDa) was used as a loading control.

SMN Expression in the Spinal Cord and Brain of SMNΔ7 Mice after i.c.v. Injection of AAV9-SYN-SMN Is Similar to That after i.v. Injection of AAV9-PGK-SMN

We previously performed two independent studies[14,20] in which we showed that the injection of an AAV9-PGK-SMN at a dose of 4.5×10^{10} vg/mouse, via either the i.v. or i.c.v. route, was sufficient to drive SMN expression in the spinal cords of SMNΔ7 mice and to rescue pathological signs of the disease.[14,20] In this study, we compared the two administration routes side by side and observed that there was significant re-expression of the SMN protein in the spinal cord and brain in both cases 2 weeks after injection relative to that detected in untreated SMNΔ7 mice (Figures S1A–S1C).

We then compared SMN expression after i.c.v. delivery of the newly generated vector to i.v. or i.c.v. delivery of AAV9-PGK-SMN. As expected, the i.c.v. administration of AAV9-PGK-SMN led to the strongest expression of SMN in CNS tissues. The quantity of SMN was 6- to 9-fold higher than that observed in the brains and spinal cords of SMNΔ7 mice injected i.c.v. with AAV9-SYN-SMN or i.v. with AAV9-PGK-SMN. Interestingly, i.c.v. delivery of AAV9-SYN-SMN at the high dose induced SMN expression in the spinal cord and brain at a comparable level to that following i.v. delivery of AAV9-PGK-SMN (Figures 2A–2C).

i.c.v. Injection of AAV9-SYN-SMN Partially Rescues the SMNΔ7 Mouse Phenotype, Extends Survival, and Increases Body Weight

We tested the effect of AAV9-SYN-SMN on the SMA phenotype by analyzing the survival of SMNΔ7 mice injected i.c.v. with the two doses of AAV9-SYN-SMN and comparing it to that of the groups of animals receiving AAV9-PGK-SMN injections. Due to insufficient levels of SMN in the spinal cord (Figure 1B), animals injected with the low dose of AAV9-SYN-SMN showed similar median and mean survival than untreated SMNΔ7 mice (median, 15.5 days versus

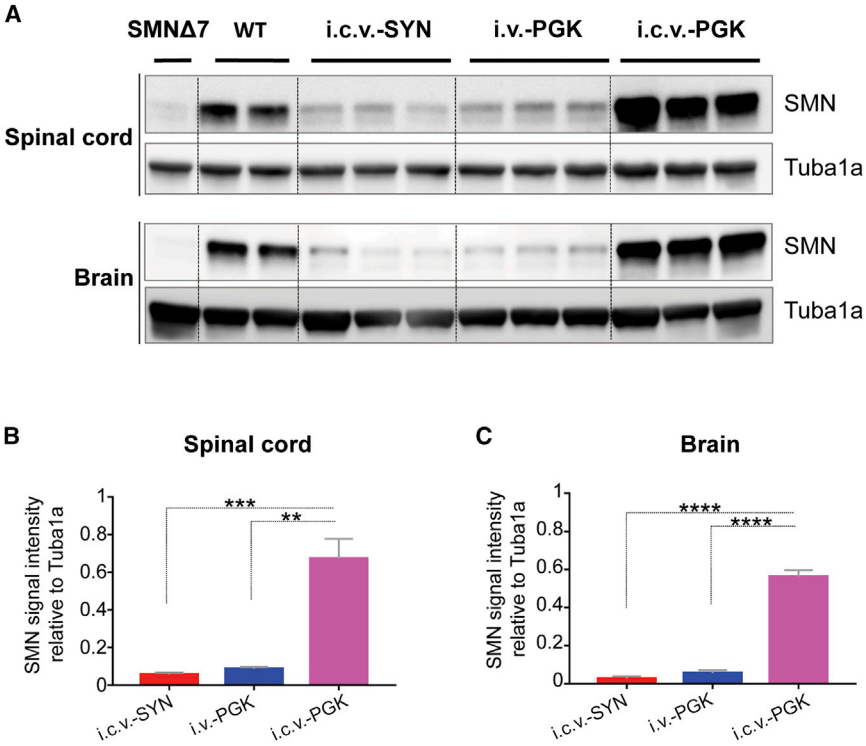

Figure 2. i.c.v. Injection of AAV9-SYN-SMN and i.v. Injection of AAV9-PGK-SMN Restores SMN Expression to Similar Levels in the Spinal Cord and Brain of SMNΔ7 Mice

(A) Western blot analyses of SMN expression (37 kDa) in the spinal cords (upper panels) and brains (lower panels) of 14-day-old SMNΔ7 mice after i.c.v. injection of AAV9-SYN-SMN (i.c.v.-SYN, n = 3) at a dose of 1.2×10^{11} vg/mouse or i.v. (i.v.-PGK, n = 3) or i.c.v. injection (i.c.v.-PGK, n = 3) of AAV9-PGK-SMN at a dose of 4.5×10^{10} vg/mouse. Protein lysates from an age-matched non-injected SMNΔ7 mouse (n = 1) and WT mice (n = 2) were used as references for SMN expression. Tuba1a (50 kDa) was used as a loading control. (B and C) Densitometric analysis of western blot signals in the spinal cords (B) and brains (C) of injected SMNΔ7 mice. Statistical analysis was performed on n = 3 mice for each group of injected mice. Significant differences in SMN expression were observed between i.c.v. injection of AAV9-PGK-SMN and either i.v. injection of the same vector or i.c.v. injection of AAV9-SYN-SMN. Values are expressed as the SMN mean intensity relative to that of Tuba1a ± SEM, and the differences between groups were analyzed by one-way ANOVA followed by Tukey's *post hoc* test (**$p < 0.01$, ***$p < 0.001$, ****$p < 0.0001$).

16.0 days, respectively) (Figures 3A and 3B; Table 1). This group was thus not analyzed further. In contrast, treatment with the high dose of AAV9-SYN-SMN (named i.c.v.-SYN high) significantly extended the lifespan of SMNΔ7 mice over that of untreated mice ($p < 0.01$), with median survival of 39.5 days (Figures 3A and 3B; Table 1). Between AAV9-PGK-SMN treatment via i.v. (i.v.-PGK) and i.c.v. (i.c.v.-PGK) administration, i.c.v. injection of AAV9-PGK-SMN resulted in the highest survival. i.v. administration of AAV9-PGK-SMN extended median survival to 126 days, whereas i.c.v.-PGK-mediated treatment extended the lifespan to 205 days, versus that of untreated SMNΔ7 mice ($p < 0.0001$ for each comparison) (Figures 3A and 3B; Table 1).

Despite the slightly improved lifespan at the high dose, i.c.v. delivery of AAV9-SYN-SMN was less efficient in terms of extending survival than was i.c.v. injection of AAV9-PGK-SMN and systemic injection of AAV9-PGK-SMN ($p < 0.0001$ and $p < 0.001$, respectively). This was surprising, as we observed similar levels of SMN in whole brain and spinal cord extracts of SMNΔ7 mice treated with i.v.-PGK and i.c.v.-SYN high (Figures 2A–2C). However, the mean survival was not statistically different between the two groups, because one mouse in the i.c.v.-SYN high group survived for 243 days, far beyond the 60 days of mean survival of the remaining 90% of the mice, increasing the standard deviation within the group.

While monitoring the treated animals over time, we observed significant differences in the overall phenotype of mice injected with the different vectors and delivery routes.

In terms of body weight, the injection of AAV9-SYN-SMN was the only treatment unable to prevent weight loss of SMNΔ7 mice during the first 3 weeks of life ($p = 0.35$). In contrast, i.c.v.- and i.v.-PGK-injected SMNΔ7 mice showed significantly higher body weight than untreated animals ($p < 0.0001$ and $p < 0.01$, respectively), although treated animals remained smaller than their heterozygous littermates. We investigated whether the weight difference between the IV-PGK and the i.c.v.-SYN treatment was due to delayed expression of SMN driven by the SYN promoter.

Analysis of SMN expression in the spinal cords of SMNΔ7 mice 1 week after i.v. injection with AAV9-PGK-SMN or i.c.v. injection with AAV9-SYN-SMN showed no significant difference between the two groups (Figure S2). Hence,no difference in the timing of expression of the two vectors was observed, suggesting better rescue upon ubiquitous SMN expression than after neuron-specific delivery during the first 3 weeks of life.

Weight comparisons among the various conditions between 4 and 10 weeks of life showed the AAV9-SYN-SMN-treated mice to follow the same growth curve as the AAV9-PGK-SMN i.v.-injected mice ($p = 0.99$). There was a significant difference in body weight between the mice injected i.c.v. with AAV9-PGK-SMN and those injected i.v. with the same viral vector ($p < 0.0001$). This difference was observed until 36 weeks of age ($p < 0.001$). Only one animal injected with AAV9-SYN-SMN survived beyond 11 weeks of age. Thus, it was not included in the statistical analysis of weight performed between 11 and 36 weeks (Figure 3C). These data show that treatment with

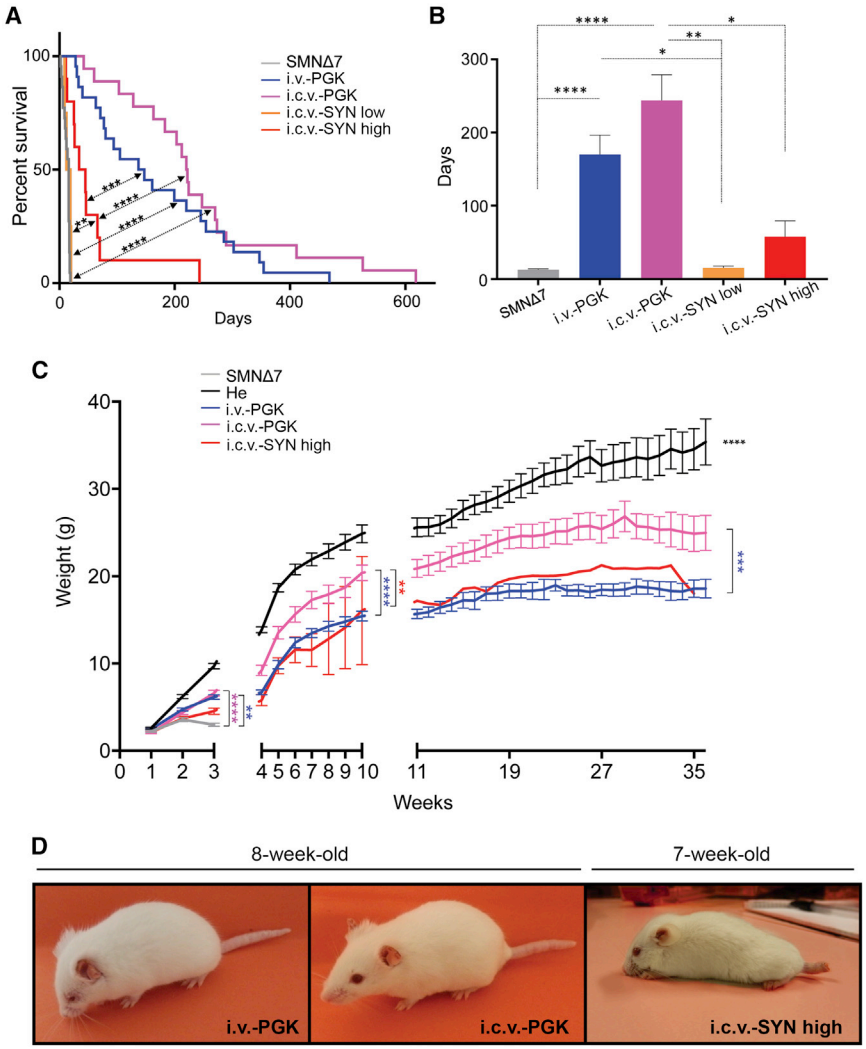

Figure 3. i.c.v. Delivery of AAV9-SYN-SMN Results in the Limited Rescue of Survival and Phenotypic Improvement of SMA Mice Relative to i.v. or i.c.v. Injection of AAV9-PGK-SMN

(A) Kaplan-Meier survival curves of SMNΔ7 mice injected i.c.v. with AAV9-SYN-SMN at a dose of 4.5×10^{10} vg/mouse (i.c.v.-SYN low, orange, n = 4) or 1.2×10^{11} vg/mouse (i.c.v.-SYN high, red, n = 10) or injected i.v. with AAV9-PGK-SMN at a dose of 4.5×10^{10} vg/mouse (i.v.-PGK, blue, n = 22) or injected i.c.v. (i.c.v.-PGK, pink, n = 18) compared to the survival curve of untreated SMNΔ7 mice (gray, n = 22). All injection methods, except i.c.v.-SYN low, significantly enhanced the lifespan of SMNΔ7 mice. The greatest lifespan was observed with the AAV9-PGK-SMN vector. No statistical difference was observed with this vector between the i.v. and i.c.v. delivery routes. The AAV9-SYN-SMN vector injected i.c.v. only offered a modest extension of lifespan when delivered at the high dose. Values are expressed as the percentage of survival, and differences between groups were analyzed using the log rank Mantel-Cox test (**$p < 0.01$, ***$p < 0.001$, ****$p < 0.0001$). (B) Bar graph showing a significant difference between the mean survival of SMNΔ7 mice (gray, n = 22) and both i.v.- and i.c.v.-injected AAV9-PGK-SMN mice at a dose of 4.5×10^{10} vg/mouse (i.v.-PGK, blue, n = 22; i.c.v.-PGK, pink, n = 18). The mean survival of i.c.v.-SYN-treated mice at either the low dose (4.5×10^{10} vg/mouse, i.c.v.-SYN low, orange, n = 4) or high dose (1.2×10^{11} vg/mouse, i.c.v.-SYN high, red, n = 10) was not significantly different from that of untreated mice, but was significantly shorter than the mean survival obtained after i.c.v. injection of AAV9-PGK-SMN. The mean survival of i.c.v.-SYN-treated mice was significantly lower than that of i.v.-injected mice with AAV9-PGK-SMN only at the low dose. No statistical difference was observed for either delivery route with AAV9-PGK-SMN. Results are expressed as the mean ± SEM, and differences between groups were analyzed using the Kruskal-Wallis test followed by Dunn's *post hoc* test (*$p < 0.05$, **$p < 0.01$, ****$p < 0.0001$). (C) Body weight curves of SMNΔ7 mice injected i.c.v. with AAV9-SYN-SMN at a dose of 1.2×10^{11} vg/mouse (i.c.v.-SYN high, red, n = 10) and injected i.v. or i.c.v. with AAV9-PGK-SMN at 4.5×10^{10} vg/mouse (i.v.-PGK, blue, n = 22; i.c.v.-PGK, pink, n = 18) compared to the body weight curves of untreated (gray, n = 22) and heterozygous (He) mice (black, n = 28). Due to early mortality in mice from the SMNΔ7, i.c.v.-SYN low, and i.c.v.-SYN high groups, the group comparisons were treated separately for three time periods: 1–3 weeks, 4–10 weeks, and 11–36 weeks. All groups were sex balanced. Data are expressed as the mean ± SEM, and differences between the curves of the i.v.-PGK, i.c.v.-PGK, i.c.v.-SYN high, and He mice were compared by two-way mixed-model ANOVA followed by Tukey's *post hoc* test (treatment and time). At 1–3 weeks (comparison between all groups), significant differences were observed between the i.c.v. and i.v. injections of AAV9-PGK-SMN but not between either i.c.v.-SYN low or i.c.v.-SYN high and the untreated SMNΔ7 mice. The He group was significantly different than all other groups. At 4–10 weeks (comparison between He, i.c.v.-PGK, i.v.-PGK, and i.c.v.-SYN high), significant differences were observed between the He mice and all injection groups and between i.c.v.-PGK and both i.v.-PGK and i.c.v.-SYN high. No difference was observed between i.v.-PGK and i.c.v.-SYN high. At 11–36 weeks (comparison between He, i.c.v.-PGK, and i.v.-PGK), significant differences were observed between all tested groups (**$p < 0.01$, ***$p < 0.001$, ****$p < 0.0001$). (D) Representative images showing the phenotype of SMNΔ7 mice injected i.v. or i.c.v. with AAV9-PGK-SMN at 8 weeks of age (left and middle, respectively) and injected i.c.v. with AAV9-SYN-SMN at 7 weeks of age (right). The SMNΔ7 mouse treated with AAV9-PGK-SMN i.v. showed reduced self-grooming, a shorter tail, and ear necrosis. The mouse injected with AAV9-PGK-SMN i.c.v. showed solely a shorter tail and ear necrosis. The i.c.v.-SYN-injected mouse showed signs of kyphosis, as well as pronounced tail necrosis.

AAV9-SYN-SMN only partially prevented the weight loss of SMNΔ7 mice.

Additionally, all mice injected with AAV9-SYN-SMN that survived beyond 6 weeks (4 of 10) looked less healthy than did those that received either the i.v.-PGK or i.c.v.-PGK treatment based on general appearance (Figure 3D; Figures S3A and S3B). In addition to ear necrosis and shorter tails, they displayed digital and tail necrosis starting from 6 weeks of age until loss, a few weeks later (Figure 3D; Figures S3A and S3B). SMNΔ7 mice injected i.v. and i.c.v. with AAV9-PGK-SMN did not show tail necrosis. However, similarly to the mice injected i.c.v. with AAV9-SYN-SMN, they developed ear necrosis (Figure 3D; Figures S3A and S3B). Despite this ear phenotype, the i.c.v.-PGK-treated mice generally appeared to be self-groomed,

Table 1. Survival Data Obtained after the Treatment of SMNΔ7 Mice with AAV9-PGK-SMN or AAV9-SYN-SMN

		Survival (Days)				
	n	Mean	SEM	Median	Minimum	Maximum
SMNΔ7	22	12.7	1.2	16.0	2	19
i.v.-PGK	22	170.0	26.6	142.0	28	468
i.c.v.-PGK	18	244.1	34.9	221.0	42	618
i.c.v.-SYN low	4	15.0	2.7	15.5	9	20
i.c.v.-SYN high	10	57.9	21.5	39.5	11	243

Survival data (mean and median) of SMNΔ7 mice injected i.v. or i.c.v. with AAV9-PGK-SMN at 4.5×10^{10} vg/mouse or injected i.c.v. with AAV9-SYN-SMN at 4.5×10^{10} vg/mouse (low) or 1.2×10^{11} vg/mouse (high) compared to that of untreated SMNΔ7 mice. N is the number of animals per group. The minimum and maximum survival levels per group are reported.

confirming that i.c.v. administration of AAV9-PGK-SMN outperforms the other delivery methods.

Overall, these observations show that SMN expression restricted to neurons induces only limited improvement in the phenotype of SMNΔ7 mice relative to that following systemic treatment.

i.c.v. Injection of AAV9-PGK-SMN Leads to Better Improvement of Neuromuscular Function and Locomotor Ability Than Other Treatments (i.v.-PGK and i.c.v.-SYN)

We assessed whether the difference in survival and phenotypic features among SMNΔ7 mice injected with the various constructs reflected neuromuscular improvement. We thus evaluated the righting reflex in i.v.-PGK-, i.c.v.-PGK-, and i.c.v.-SYN high-treated juvenile SMNΔ7 mice (Figure 4). The general body strength, measured within the first 3 weeks of life, was restored in all groups of injected SMNΔ7 mice. However, it never reached the same level as that of the control heterozygous mice ($p < 0.0001$ for all comparisons). SMNΔ7 mice treated with i.c.v.-PGK showed the best ability to right themselves relative to both i.v.-PGK- and i.c.v.-SYN-injected mice ($p < 0.0001$ and $p < 0.001$, respectively). Animals treated with i.v.-PGK and i.c.v.-SYN high were indistinguishable, showing an identical righting response ($p = 0.99$). This suggests that comparable levels of SMN in the spinal cord induce similar effects on body strength in the first weeks of life.

We further analyzed the functional behavior of the mice treated via the different injection routes by measuring motor coordination using the rotarod test during the third month of life. At this point, all i.c.v.-SYN high-treated mice were dead. Among the remaining cohorts, motor function was restored only in SMNΔ7 mice injected with i.c.v.-PGK (Figure 5A). These mice spent an average of 60 s on the wheel, similarly to heterozygous mice (61 ± 5 s versus 63 ± 6 s). The i.v.-PGK-injected animals lasted half that time on the rotating rod. This was significantly different than both the heterozygous and i.c.v.-PGK-treated mice (28 ± 4 s; $p < 0.001$ and $p < 0.01$ compared to heterozygous and i.c.v.-PGK-treated mice, respectively).

We also evaluated the therapeutic efficacy of the treatments by analyzing the spontaneous motor activity of injected SMNΔ7 mice and control heterozygous animals using an actimeter (Figures 5B and 5D). Remarkably, i.c.v.-PGK-treated animals behaved similarly to heterozygous mice for the global movement and distance covered analysis (2,151 ± 173 s and 83 ± 14 m for i.c.v.-PGK-injected animals versus 2,472 ± 105 s and 129 ± 14 m for heterozygous mice) (Figures 5B and 5C), whereas i.v.-PGK-treated mice moved less in the cage and walked a shorter distance than heterozygous mice (1,688 ± 216 s and 65 ± 14 m for global movement and distance covered; $p < 0.01$ and $p < 0.05$, respectively). Additionally, the number of rearings was statistically lower in mice treated with either delivery route than those of heterozygous mice (111 ± 27 for i.v.-PGK-injected animals and 464 ± 57 for i.c.v.-PGK-injected animals versus 783 ± 44 for heterozygous mice; $p < 0.0001$ and $p < 0.001$ for i.v.-PGK- and i.c.v.-PGK-injected mice compared to heterozygous animals, respectively), but significantly higher for i.c.v.-PGK than systemically treated mice ($p < 0.01$) (Figure 5D). These analyses further confirm that the i.c.v. administration of AAV9-PGK-SMN outperforms systemic delivery of the same vector.

i.c.v. Injection of AAV9-SYN-SMN Efficiently Transduces MNs at Higher Levels Than i.v. Administration of AAV9-PGK-SMN

We hypothesized that the limited survival observed in SMNΔ7 mice injected i.c.v. with AAV9-SYN-SMN relative to that of systemically treated mice, despite similar global levels of SMN protein (Figures 2A–2C), could be explained by different transduction levels in spinal MNs. We thus compared the expression of SMN in the MNs of i.c.v.-SYN-injected mice to that in the MNs of i.v.-PGK or i.c.v.-PGK mice at 14 days of life.

Double immunofluorescence analyses of spinal-cord sections using antibodies against SMN and choline acetyltransferase (ChAT) (a marker for MNs) were performed in the lumbar and cervical spinal cord tracts (Figure 6; Figure S4). SMN was expressed in far fewer $ChAT^+$ cells (9.41% ± 2.47% in lumbar sections and 6.97% ± 1.63% in cervical sections) of SMNΔ7 mice than those of wild-type (WT) mice (94.32% ± 1.85% in lumbar sections and 93.53% ± 1.42% in cervical sections) (Figures 6A–6F and 6P; Figures S4A–S4F and S4P). In WT mice, the signal for SMN was mainly located in the gems of MN nuclei (Figures 6D–6F; Figures S4D–S4F). In contrast, we observed staining both in the nuclei and cytoplasm of transduced cells in all injected SMNΔ7 mice in which SMN was overexpressed (Figures 6G–6O; Figures S4G–S4O). As expected, upon i.c.v.-PGK injection, a high percentage of $ChAT^+$ cells were transduced (99.58% ± 0.42% in lumbar sections and 99.84% ± 0.16% in cervical sections) (Figures 6J–6L and 6P; Figures S4J-S4L and S4P).

Among the three treatments, i.v.-PGK administration resulted in the lowest percentage of SMN/$ChAT^+$ cells (46.56% ± 3.03% in lumbar sections and 57.77% ± 6.53% in cervical sections) (Figures 6G–6I and 6P; Figures S4G–S4I and S4P), whereas i.c.v.-SYN injection transduced 80% of MNs (84.29% ± 3.12% in lumbar sections and 73.06 ± 4.90% in cervical sections) (Figures 6M–6P; Figures S4M–S4P).

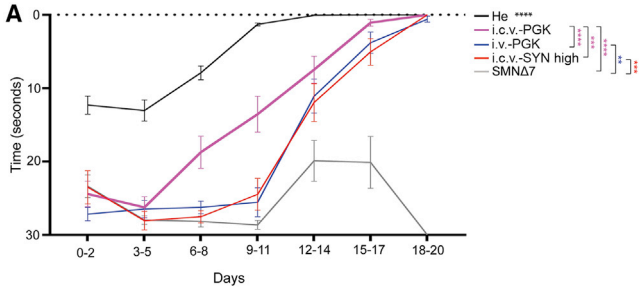

Figure 4. Injection of Either AAV9-PGK-SMN or AAV9-SYN-SMN Restores the Righting Reflex in SMNΔ7 Juvenile Mice

(**A**) The righting reflex was assessed daily in SMNΔ7 mice injected i.v. (i.v.-PGK, blue, n = 14) or i.c.v. (i.c.v.-PGK, pink, n = 12) with AAV9-PGK-SMN at a dose of 4.5×10^{10} vg/mouse or in i.c.v.-SYN-injected (i.c.v.-SYN high, n = 10) SMNΔ7 mice and compared to that of untreated SMNΔ7 mice (gray, n = 22) and He mice (black, n = 35) from birth to postnatal day 20. Data are expressed as the mean every 3 days ± SEM. Significant statistical differences were observed between all compared groups except for the comparison between i.v.-PGK- and i.c.v.-SYN high-injected mice. Differences between the curves were analyzed by two-way mixed model ANOVA followed by Tukey's *post hoc* test (treatment and time) (**$p < 0.01$, ***$p < 0.001$, ****$p < 0.0001$).

We further verified the effect of the treatments in protecting MNs by quantifying the total number of $ChAT^+$ cells in lumbar and cervical sections of treated and untreated SMNΔ7 and WT mice (Figure 6Q; Figure S4Q). As expected, SMNΔ7 mice showed a lower number of MNs than WT mice (8.42 ± 0.54 and 10.87 ± 0.46 in the lumbar and cervical sections of SMNΔ7 mice, respectively, versus 11.5 ± 0.65 and 15.33 ± 0.31 in the lumbar and cervical sections of WT mice, respectively; $p < 0.01$ and $p < 0.0001$, respectively). Consistent with the higher expression of SMN, i.c.v.-PGK-injected mice showed a higher number of MNs in both lumbar (11.31 ± 0.86) and cervical (13.56 ± 0.51; $p < 0.01$) sections than untreated SMNΔ7 mice, reaching an amount comparable to that of WT mice. In contrast, there was no statistically significant difference in the number of MNs in the spinal cords of i.v.-PGK-injected mice (8.50 ± 0.70 and 10.59 ± 0.34 in lumbar and cervical sections, respectively) or those injected i.c.v. with AAV9-SYN-SMN (9.31 ± 0.41 and 12.48 ± 0.47 in lumbar and cervical sections, respectively) relative to SMNΔ7 mice. Furthermore, the number of $ChAT^+$ cells was similar in both the lumbar and cervical spinal cords of SMNΔ7 mice injected i.v. with AAV9-PGK-SMN and injected i.c.v. with AAV9-SYN-SMN, indicating a similar effect on MN survival following the administration of the two vectors.

We further analyzed the distribution of re-expressed SMN among the cell types resident in the spinal cord, such as astrocytes. We could not detect any SMN signal in glial fibrillary acid protein (GFAP)-positive cells upon i.c.v. injection of the AAV9-SYN-SMN vector, confirming the specificity of the construct for neurons (Figure S5). However, i.v.-PGK treatment very rarely transduced astrocytes, suggesting that the differences observed between these two treatments were very unlikely determined by SMN restoration in astrocytes and rather that other cell types may be involved. As expected, the i.c.v. injection of AAV9-PGK-SMN resulted in higher expression of SMN in astrocytes than that following i.v. delivery, but only a few positive astrocytes were detected.

i.v. and i.c.v. Administration of AAV9-PGK-SMN Restores SMN Expression in Peripheral Organs

We reasoned that the better survival and phenotypic rescue observed in i.v.-PGK-treated SMNΔ7 mice than i.c.v.-SYN mice could be the result of SMN expression in peripheral organs.

Therefore, we assessed SMN protein levels in whole lysates from skeletal muscle, heart, and liver from SMNΔ7 mice injected i.v. or i.c.v. with AAV9-PGK-SMN or control animals at 14 days (Figures 7A–7D). As in the CNS, SMN protein levels were almost undetectable in the peripheral organs of SMNΔ7 mice. The SMN signal in WT mice was approximately 3-, 6-, and 8-fold higher in the heart, muscle, and liver, respectively, than in SMNΔ7 mice. AAV9-PGK-SMN injection by either the i.v. or i.c.v. routes restored SMN levels similar to those of WT mice in the three organs. In contrast to the CNS, i.v.-PGK treatment resulted in similar SMN expression as that of i.c.v.-injected mice for all three analyzed organs (Figures 2D and 7B–7D).

Finally, we investigated whether the exogenous SMN was differentially localized in the heart and liver of i.v.- and i.c.v.-injected mice by assessing its expression by anti-SMN immunofluorescence (Figures 7E–7L). We observed similar localization of the protein in the cytoplasm of cardiac and hepatic cells with both delivery routes.

DISCUSSION

Our goal was to understand whether selective expression of SMN in neurons can provide a therapeutic effect in SMNΔ7 mice. We thus generated a novel AAV9-SMN construct expressing SMN under the control of the human SYN promoter. We also performed a comprehensive comparison of this approach with previously tested gene therapy treatments using an AAV9 expressing SMN under the control of the ubiquitous promoter PGK. We show that AAV9-mediated replacement of SMN in neurons using AAV9-SYN-SMN is not sufficient to rescue the SMA phenotype in SMNΔ7 mice. In contrast, the i.v. administration of AAV9-PGK-SMN resulted in better survival and phenotypic improvement of SMNΔ7 mice, even though the levels of SMN protein in the CNS organs and MN transduction were similar to those found after AAV9-SYN-SMN injection. The most efficient rescue of SMNΔ7 mice was, however, obtained by i.c.v. injection of AAV9-PGK-SMN, confirming our previous results.[45] This approach led to higher expression of SMN in CNS tissues and levels in peripheral organs similar to those in WT mice. Elevated expression of SMN in the spinal cord fully protected MNs, albeit survival and functional studies revealed that the animals were not rescued to the extent of heterozygous mice.

Overall, these results, summarized in Figure 8, confirm that SMN expression in neurons is necessary but not sufficient for the complete recovery of SMNΔ7 mice, suggesting that optimization is nevertheless needed to develop efficient gene replacement approaches for SMA.

Gene therapy is an attractive therapeutic option for SMA patients. It can provide stable and long-term correction of the faulty gene with a single dose.[55–57] Pre-clinical studies have demonstrated that it is possible to rescue SMNΔ7 mice using lower doses of AAV9-SMN

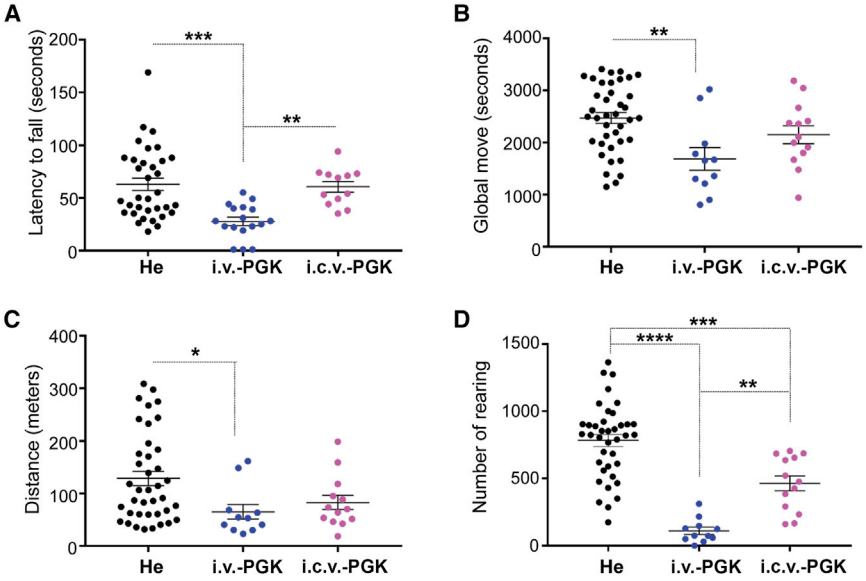

Figure 5. i.c.v. Injection of SMNΔ7 Mice with AAV9-PGK-SMN Provides Better and Sustained Protection of Locomotor Functions than Does Systemic Delivery

(A) The rotarod performance of SMNΔ7 mice injected i.v. (i.v.-PGK, blue dots, n = 17) or i.c.v. (i.c.v.-PGK, pink dots, n = 12) with AAV9-PGK-SMN at a dose of 4.5×10^{10} vg/mouse and He mice (black dots, n = 34) was assessed daily from 10 weeks of age. Mice were trained for 10 days and the rotarod performance was recorded during the next 10 days. Data are expressed as the mean ± SEM. Differences between groups were analyzed by the Kruskal-Wallis test followed by Dunn's *post hoc* test (**$p < 0.01$, ***$p < 0.001$). (B–D) Spontaneous motor activity monitored during 1 h using an actimeter for SMNΔ7 mice injected i.v. (i.v.-PGK, blue dots, n = 11) or i.c.v. (i.c.v.-PGK, pink dots, n = 13) with AAV9-PGK-SMN and He controls (black dots, n = 39) at 12 weeks of age. Overall time spent moving (B), the covered distance (C), and the number of rearings (D) were recorded. Data are expressed as the mean ± SEM. Differences between groups were analyzed by one-way ANOVA followed by Tukey's *post hoc* test (*$p < 0.05$, **$p < 0.01$, ***$p < 0.001$, ****$p < 0.0001$).

when it is administered into the CSF, e.g., by i.c.v. injection, than by i.v. injection.[20,22] The i.c.v. delivery route is considered to be better for vector administration, as it efficiently targets the CNS, avoiding peripheral dispersion of the vector, and consequently requires a lower viral dose than i.v. injection.[20–29] Indeed, a dose-dependence study using an AAV9 vector carrying SMN under the control of the ubiquitous chicken-β-actin promoter showed that lower doses of the vector were needed for i.c.v. injection to attain similar efficiency than previously tested systemic injection.[22] A similar method is currently being used in a clinical trial for the treatment of SMA patients following intrathecal administration (as a translation of intra-CSF delivery) (ClinicalTrials.gov: NCT03381729). Furthermore, the splice-switching antisense oligonucleotide Spinraza is administered through repeated intrathecal injections to SMA patients.[58,59] However, it is still unknown whether these approaches will restore sufficient levels of SMN in both the CNS and periphery and mediate long-lasting therapeutic effects in treated patients. Therefore, understanding in which tissues SMN expression is required is pivotal for the design of optimal treatments based on SMN expression. We anticipate that pre-clinical studies addressing this issue will help to predict clinical outcomes and the management of treated SMA patients.

Our work stems from the growing evidence challenging the vision of SMA as a pure MN disease. Defects in several peripheral tissues have been identified in animal models and human samples from patients with the most severe form of SMA, highlighting multi-systemic impairment as an important pathological component (reviewed in Hamilton et al.,[30] Nash et al.,[31] and Shababi et al.[32]). Several transgenic mouse models have been generated to specifically delete or re-express SMN in the CNS or peripheral tissues to better understand its tissue-specific contribution. For example, SMN expression in the CNS using the prion promoter led to strong phenotypic rescue in SMA mice, stressing the importance of SMN re-expression in neurons.[60] However, the prion promoter also induces a low level of SMN expression outside the CNS, such as in the heart, kidneys, and skeletal muscle, which likely contributed to the reported phenotypic improvement.[61] Another study reported that *Smn* depletion restricted to motor neural progenitors, using *Olig2*-Cre mice, only led to a mild SMA phenotype, probably due to a protective role played by *Smn* expressed in other tissues.[62] Furthermore, two independent studies have demonstrated the central role of SMN in skeletal muscle, underscoring the need to ensure SMN expression in the periphery to restore proper motor function.[33,60]

We reasoned that postnatal overexpression of SMN restricted to neurons, using AAV9 vectors, would be a straightforward method to study the requirement of SMN expression in other tissues. We took advantage of the previously described human SYN promoter, which was already been proven to be selective for targeting neurons.[51–53] Although leakage in the liver was previously reported,[63] we did not observe SMN expression in the skeletal muscle, heart, liver, or astrocytes of treated mice. This could be ascribed to the dose of AAV9 used in our study, which was sufficient to drive expression in neurons but limited the nonspecific targeting of other cell types.

We compared the effects of neuron-specific SMN expression to the i.v. or i.c.v. delivery of our previously developed therapeutic vector AAV9-PGK-SMN.[14,20] A 3-fold higher dose of AAV9-SYN-SMN was necessary to express SMN at levels similar to those following systemic injection of AAV9-PGK-SMN in the spinal cord. Accordingly, we only observed improvement of SMNΔ7 mouse survival when AAV9-SYN-SMN was administered at a high dose. The extension of survival was modest relative to that following i.v. or i.c.v. administration of AAV9-PGK-SMN, allowing similar or higher SMN expression than in WT mice in the CNS organs and MNs, respectively.

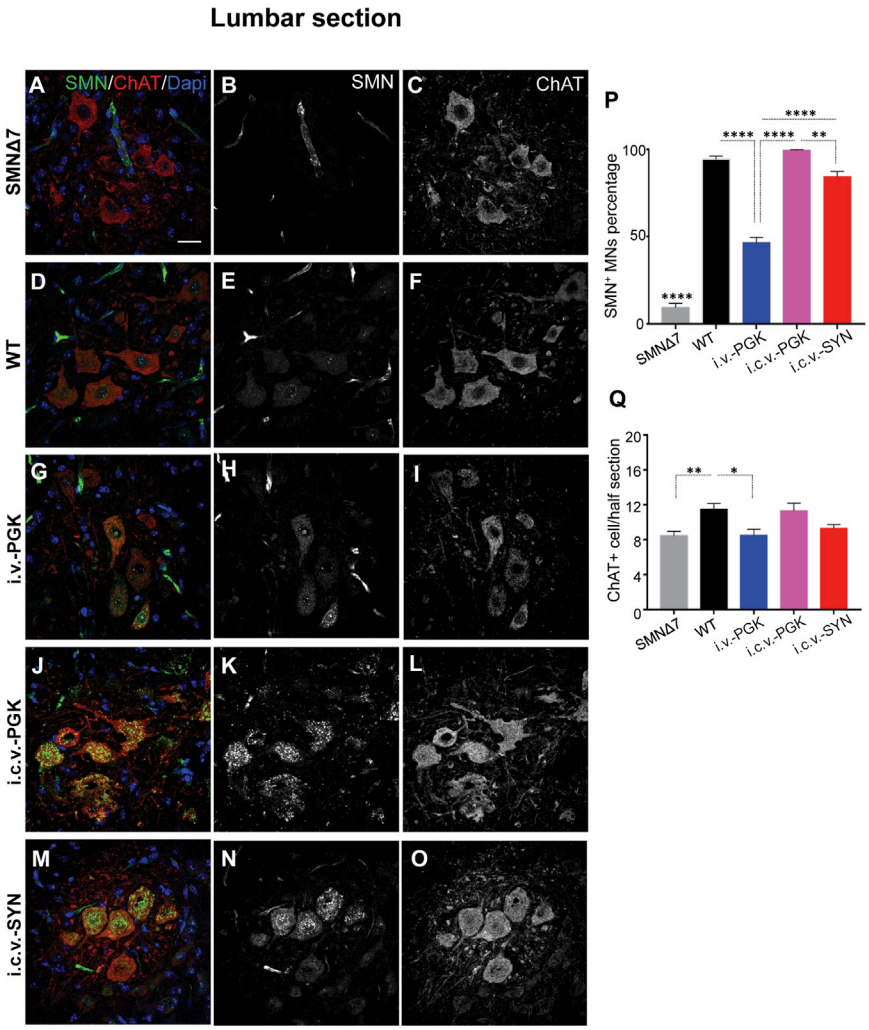

Figure 6. SMN Transduction in MNs of the Lumbar Spinal Cord Is Higher in i.c.v.-SYN Mice Than in Systemically Treated SMNΔ7 Mice

(A–O) Representative transverse sections of the ventral horn of the lumbar spinal cord from SMNΔ7 mice injected i.v. (i.v.-PGK, G–I) or i.c.v. (i.c.v.-PGK, J–L) with AAV9-PGK-SMN at a dose of 4.5×10^{10} vg/mouse; SMNΔ7 mice injected i.c.v. with AAV9-SYN-SMN at 1.2×10^{11} vg/mouse (i.c.v.-SYN, M–O); untreated SMNΔ7 mice (A–C); and WT mice (D–F). Sections were processed for ChAT/SMN double immunofluorescence (green, SMN^+ cells, red, $ChAT^+$ cells) at 14 days of age. Nuclei were stained with DAPI (blue). Single SMN staining (gray) is presented in (B), (E), (H), (K) and (N). Single ChAT staining (gray) is presented in (C), (F), (I), (L), and (O). Scale bar, 25 μm. (P) Percentage of SMN^+ MNs per section of 14-day-old SMNΔ7 mice injected i.v. (i.v.-PGK, blue, n = 3) or i.c.v. (i.c.v.-PGK, pink, n = 3) with AAV9-PGK-SMN at a dose of 4.5×10^{10} vg/mouse and SMNΔ7 mice injected i.c.v. with AAV9-SYN-SMN at a dose of 1.2×10^{11} vg/mouse (i.c.v.-SYN, red, n = 3). Age-matched non-injected SMNΔ7 mice (gray, n = 3) and WT mice (black, n = 4) were used as references. Data are expressed as mean percentage ± SEM and differences between groups were analyzed by one-way ANOVA followed by Tukey's *post hoc* test (**$p < 0.01$, ****$p < 0.0001$). (Q) Quantitative analysis of the number of $ChAT^+$ MNs of 14-day-old SMNΔ7 mice injected i.v. (i.v.-PGK, blue, n = 3) or i.c.v. (i.c.v.-PGK, pink, n = 3) with AAV9-PGK-SMN at a dose of 4.5×10^{10} vg/mouse and SMNΔ7 mice injected i.c.v. with AAV9-SYN-SMN at a dose of 1.2×10^{11} vg/mouse (i.c.v.-SYN, red, n = 3). Age-matched non-injected SMNΔ7 mice (gray, n = 6) and WT mice (black, n = 6) were used as references. Approximately 25 sections per mouse were scored. Data are expressed as the mean ± SEM. Differences between groups were analyzed by one-way ANOVA followed by Tukey's *post hoc* test (*$p < 0.05$, **$p < 0.01$).

Although the i.c.v. administration of AAV9-SMN vectors is more effective at lower doses than i.v. delivery, a comprehensive comparison of the two delivery routes in the same setting has not yet been performed. Surprisingly, the side-by-side comparison did not reveal a significant difference in survival after the i.v. or i.c.v. injection of AAV9-PGK-SMN at the same dose. However, the longest median survival and maximal survival of SMNΔ7 mice were achieved following i.c.v. delivery of AVV9-PGK-SMN (221 days and 618 days, respectively). Importantly, a 36-week follow-up assessing the body weight of the mice showed that no cohort of treated mice reached a weight similar to that of heterozygous mice, demonstrating that even the i.c.v.-mediated, ubiquitous expression of SMN is not sufficient to fully rescue SMNΔ7 mice.

Analysis of the righting reflex showed the i.v. injection of AAV9-PGK-SMN and i.c.v. injection of AAV9-SYN-SMN to result in similar outcomes during the first weeks after treatment, but the lifespan of the SYN-SMN-treated mice was not long enough for further functional analysis (e.g., rotarod, actimeter). Comparison among the survivor groups in the adult stage showed higher performance of the SMNΔ7 mice injected i.c.v. with AAV9-PGK-SMN. These mice spent a similar amount of time in global movement and covered a similar distance as did the heterozygous control mice. Despite the significant increase in mean survival, mice that were injected i.v. with AAV9-PGK-SMN performed significantly worse than the control mice. These analyses show, for the first time, that mice treated i.c.v. with AAV9-PGK-SMN preserve locomotor abilities long after treatment.

The limited rescue observed for SMNΔ7 mice treated with AAV9-SYN-SMN could be due to insufficient targeting of the MNs. However, immunofluorescence analyses of spinal cords from treated and control mice showed that i.c.v. injection of AAV9-SYN-SMN mediated SMN expression in ~80% of MNs in both the cervical and lumbar spinal cord tracts. Based on the results reported in Passini et al.,[23] such MN transduction should have been sufficient to rescue survival and the neuromuscular phenotype of SMNΔ7 mice. However, in that study, AAV9-mediated expression of SMN was induced using the

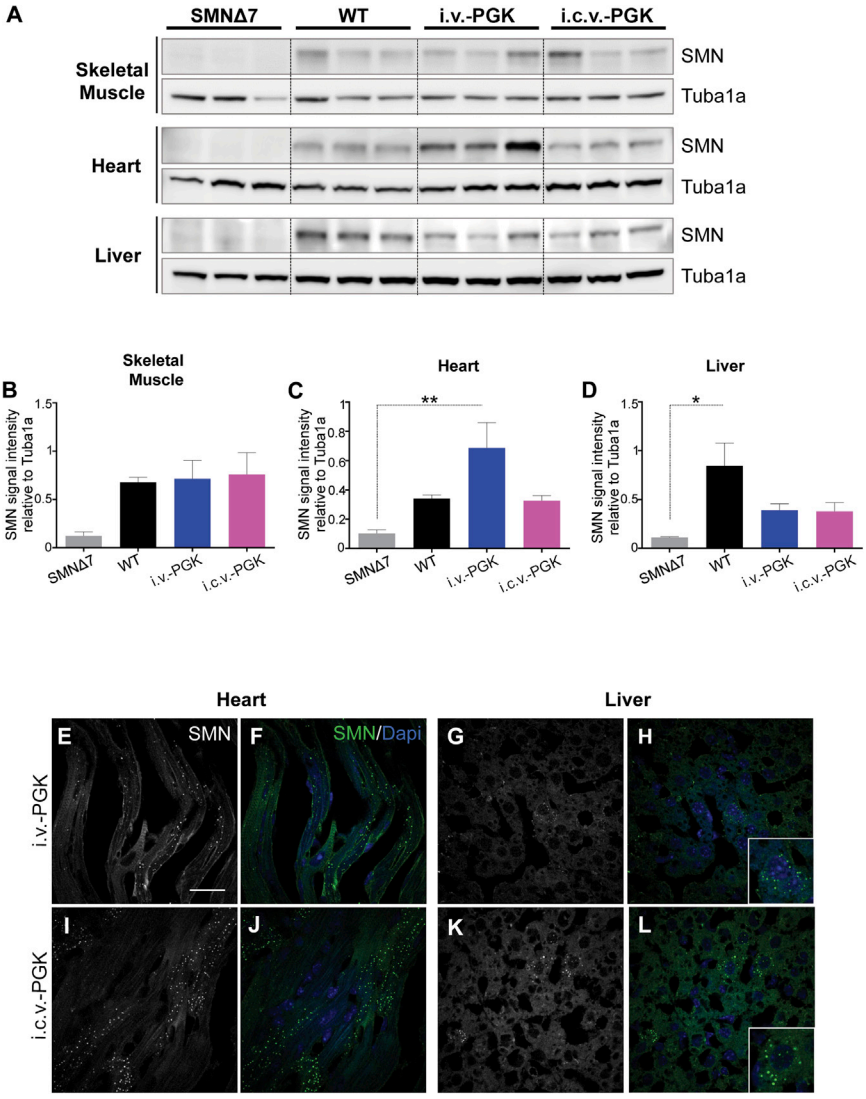

Figure 7. i.v. or i.c.v. Injection of AAV9-PGK-SMN Restores SMN Expression in Peripheral Organs to Similar Levels

(A) Western blot analyses of SMN expression (37 kDa) in skeletal muscle (upper panel), heart (middle panel), and liver (lower panel) of 14-day-old SMNΔ7 mice injected i.v. (i.v.-PGK, n = 3) or i.c.v. (i.c.v.-PGK, n = 3) with AAV9-PGK-SMN at 4.5×10^{10} vg/mouse. Age-matched non-injected SMNΔ7 mice (n = 3) and WT mice (n = 3) were used as references for SMN expression. Tuba1a (50 kDa) was used as a loading control. (B–D) Densitometry analysis of western blot results of skeletal muscle (B), heart (C), and liver (D), showing levels of SMN in i.v.- or i.c.v.-injected mice and similar to those of WT animals. Values are expressed as the SMN mean signal intensity relative to that of Tuba1a ± SEM. The differences between groups were analyzed by one-way ANOVA followed by Tukey's *post hoc* test (*$p < 0.05$, **$p < 0.01$). (E–L) Representative sections of heart (E, F, I, and J) and liver (G, H, K, and L) from SMNΔ7 mice after i.v. (E–H) or i.c.v. (I–L) injection of AAV9-PGK-SMN processed for immunofluorescence at 14 days of age using an anti-SMN antibody (green). Nuclei were stained by DAPI (blue). SMN-positive staining is presented alone (gray, E, G, I, and K) or combined with DAPI (green and blue, respectively; F, H, J, and L). Scale bar, 25 μm. A 2-fold magnification of liver cells is shown in the lower right corner of (H) and (L).

human β-glucuronidase promoter, reported to target both neurons and astrocytes.[64] Interestingly, when SMN expression was selectively directed to astrocytes using the GFAP promoter and an AAV9 vector, the survival of SMNΔ7 mice improved, although modestly.[65] It is thus possible that the positive effects of the AAV9-PGK-SMN vector on the SMNΔ7 mice were determined by the combined transduction of MNs and astrocytes. However, our immunofluorescence analyses showed that GFAP-positive astrocytes were very weakly transduced, even after i.v.-PGK treatment, suggesting that other cells contributed to the overall rescued phenotype.

These results underscore the importance of considering neurons and non-neural cells for the pathology of SMA and therapeutic applications.

Particular attention should be paid to the physiological role of SMN. Upon AAV-mediated SMN overexpression, we observed different protein localization in MNs than in WT mice by immunofluorescence. To enable SMN to properly exert its physiological role, it may be necessary to develop therapeutic approaches that can restore SMN expression at the correct levels and in the proper subcellular compartments.[66]

Our study further shows that, even in the presence of similar levels of SMN expression and MN protection in the spinal cord, the survival of SMNΔ7 mice is not restored to the same level as for mice systemically treated with the AAV9 vector expressing SMN under control of the PGK promoter. As expected, this delivery route led to SMN expression in peripheral tissues that was surprisingly similar to that observed after i.c.v. injection of the same vector.

Overall, these data emphasize the importance of SMN in organs and tissues other than the CNS. Further research is needed to define the requirements for SMN in each compartment. Studies that combine AAV vector targeting properties, specific promoters, and dose-escalation studies in SMNΔ7 mice or other relevant SMA mouse models could address these questions.[67,68] In addition, studies in animal models will only partially predict the results in humans, as SMN requirements may vary among species.[22] We speculate that the use of SMA patient-derived organoids,[69] combined with gene therapy approaches, could open concrete perspectives for understanding the contribution of SMN in different tissues.

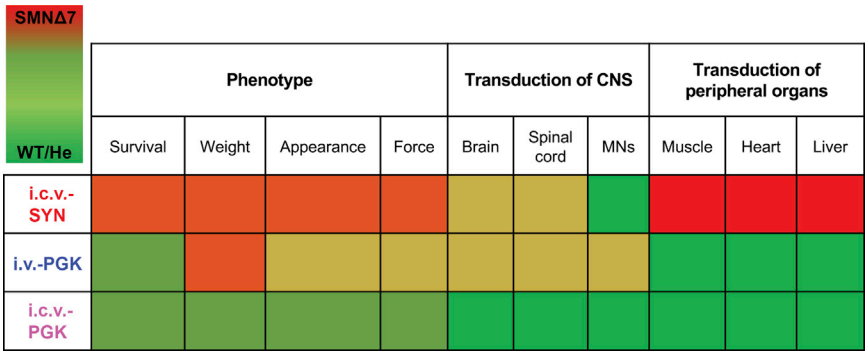

Figure 8. Graphical Summary of the Main Findings of the Study

The effects of each treatment (i.c.v.-SYN, i.v.-PGK, and i.c.v.-PGK) on the phenotype (survival, body weight, general appearance, and neuromuscular functions) are classified according to a color code, in which brilliant red and brilliant green correspond to SMNΔ7 and WT/He mice, respectively. The effects on the phenotype are compared to transduction of CNS (brain, spinal cord, and MNs) and peripheral organs (skeletal muscle, heart, and liver). SMN expression restricted to neurons (i.c.v.-SYN) mediates a modest improvement of the SMNΔ7 mouse phenotype. SMN expression in the peripheral organs contributes to a better rescue of the phenotype (i.v.-PGK and i.c.v.-PGK). High expression of SMN in both CNS tissues and peripheral organs results in the best rescue of SMA mice (i.c.v.-PGK), which are still not comparable to WT or He mice. This work highlights the importance of SMN expression in the CNS and peripheral organs for complete rescue of the SMNΔ7 phenotype.

MATERIALS AND METHODS

Animals

To obtain SMA mice, breeding pairs of triple mutant mice (*SMN2*$^{+/+}$, *SMNΔ7*$^{+/+}$, *Smn*$^{+/-}$; no. SN 5025) were purchased from The Jackson Laboratory. These mice harbor two transgenic alleles (the entire human *SMN2* gene and the human *SMN2* cDNA, lacking exon 7) and are heterozygously invalidated for the endogenous murine *Smn* gene (through lacZ reporter gene insertion into exon 2).[15] The genotype of the offspring can be WT (*SMN2*$^{+/+}$, *SMNΔ7*$^{+/+}$, *Smn*$^{+/+}$), heterozygous (*SMN2*$^{+/+}$, *SMNΔ7*$^{+/+}$, *Smn*$^{+/-}$), or knockout, named SMNΔ7 (*SMN2*$^{+/+}$, *SMNΔ7*$^{+/+}$, *Smn*$^{-/-}$). SMNΔ7 mice progressively lose body weight, starting from 5 days, and have a mean survival of approximately 14 days. To reduce the amount of breeding required for the study, heterozygous mice were used as the reference for survival, body weight, and behavioral analyses, whereas WT mice were used as the reference for biochemical and immunochemistry analyses. Heterozygous and WT animals did not show any differences in terms of life expectancy and locomotor behavior.

Mice were housed under controlled conditions following the French and European guidelines for the use of animal models (2010/63/EU).

AAV Vector Production

The expression sequence for codon-optimized human *SMN1*[14] under control of either the ubiquitous PGK promoter or the neuro-specific human SYN promoter was cloned by enzymatic restriction into the previously described deleted ITR2[70] of the AAV genome. Our group previously produced the PGK construct.[14] To obtain the AAV-SYN-SMN genome, we replaced the PGK sequence with the SYN promoter. This sequence derives from a pDrive plasmid (kind gift from Genethon-Evry), encoding a previously published sequence[51] of 469 nt plus the downstream 82 nt of the human SYN1 promoter (NG.008437.1). The two corresponding recombinant serotype 9 AAV vectors were produced using helper virus-free transient transfection in HEK293 cells following the protocol described by Biferi et al.[71] Each production was quantified by real-time PCR and vector titers were expressed as vg/mL.

In Vivo AAV Injection

Injections of new-born mice (PND1) were performed using a 50-μL Hamilton syringe with a 31G and 30-mm length needle. A total volume of 70 μL, containing 4.5×10^{10} vg of AAV vector (corresponding to 3×10^{13} vg/kg) diluted in PBS, was delivered to the temporal veins through bilateral i.v. injection (35 μL per site). Approximately 7 μL of viral suspension, containing 4.5×10^{10} or 1.2×10^{11} vg (corresponding to 8×10^{14} vg/kg, high dose), was administered into the brain lateral ventricles through a unilateral i.c.v. injection (1 mm anterior, ±1 mm lateral to the lambda, and 2 mm deep).

Histology and Immunostaining Analysis

Mice were euthanized 14 days post-injection for SMN expression analyses by intraperitoneal anesthetic injection (10 mg/kg xylazine, 100 mg/kg ketamine), followed by intracardiac perfusion, first with 1× PBS and then 4% paraformaldehyde (PFA) in PBS. Tissues were isolated and postfixed by incubation for 24 h in 4% PFA at 4°C. Brain and non-nervous organs were then incubated at least 24 h in a PBS-sucrose solution (15%) at 4°C; spinal cords were incubated in a PBS-sucrose solution (30%) under the same conditions. Dehydrated tissues were embedded in Tissue-Tek OCT and frozen in cold isopentane at a temperature between −45°C and −55°C. Serial sections of different thickness were cut using a cryostat (Leica), depending on the organ (16 μm for brains, 14 μm for spinal cords and hearts, 10 μm for livers) and were stored at −80°C.

For immunofluorescence detection of SMN in tissues, sections were permeabilized in 0.1% Triton X-100 (Bio-Rad) in PBS. Antigen retrieval was then performed in citrate buffer (10 mM citric acid, pH 6) at 95°C. After cooling and washing in PBS, sections were incubated for 1 h in blocking solution containing 4% BSA (immunoglobulin G [IgG]-free, protease-free, The Jackson Laboratory), 4% normal donkey serum (Millipore), and 0.1% Triton X-100 in PBS. A mouse anti-SMN (1:3,000; BD Biosciences) primary antibody was used in blocking solution overnight at 4°C. For MN or astrocyte staining, goat anti-ChAT (1:75; Millipore) or rabbit anti-GFAP (1:1,000;

Dako), respectively, were added to the blocking buffer for double immunofluorescence. After washing, sections were incubated with the appropriate fluorescent-conjugated secondary antibody: donkey anti-mouse Alexa Fluor 488 (1:1,000; Thermo Fisher Scientific), donkey anti-goat Alexa Fluor 594 (1:750; Thermo Fisher Scientific), or donkey anti-rabbit Alexa Fluor 594 (1:1,000; Thermo Fisher Scientific).

Nuclei were stained with DAPI (Sigma-Aldrich). Sections were mounted with FluoroMount-G mounting medium (Interchim), and the images were captured using a Leica confocal imaging system or Zeiss spinning confocal imaging system.

MN Quantification and SMN Level Assessment

$ChAT^+$ MNs (with a diameter >20 μm) were manually counted in the gray matter of whole spinal cord serial sections (approximately 24 sections per animal, n = 3 for injected animals and n = 6 for WT and SMNΔ7 animals). SMN^+ MNs were scored in the same sections (n = 3 for injected and SMNΔ7 animals and n = 5 for WT animals). The percentage of SMN-expressing MNs was assessed relative to the total number of MNs counted.

Western Blot Analyses

Protein extracts were prepared from snap-frozen tissues of PBS intracardially perfused mice. Tissues were lysed in radioimmunoprecipitation assay (RIPA) buffer (150 mm NaCl, 50 mm Tris-HCl, 0.5% sodium deoxycholate, 1% Nonidet P-40 [NP-40], 0.1% SDS) supplemented with a protease inhibitor cocktail (Complete Mini, Roche Diagnostics). Protein lysates (30 μg for spinal cord and muscles, 40 μg for brain, and 60 μg for liver and heart) were run on 10% SDS polyacrylamide gels and transferred to Immobilon-P membranes (Millipore). The membranes were then incubated with a mouse anti-SMN antibody (1:1,000; BD Biosciences) and a mouse anti-α-tubulin antibody (1:10,000; Sigma) diluted in TBST blocking buffer (Tris-buffered saline containing 0.2% Tween 20) supplemented with 5% non-fat dry milk. After several washes in TBST buffer, the membranes were incubated with a horseradish peroxidase-conjugated anti-mouse antibody (1:10,000; GE Healthcare) diluted in the blocking buffer. The membranes were further processed using the chemiluminescence SuperSignal Ultra reagent (Pierce).

Behavioral Analyses

Body weight was assessed daily until 1 month of age and once a week thereafter.

Righting Reflex

The righting reflex of mice treated with i.v.-PGK (i.v.-PGK, n = 14) or i.c.v.-PGK (n = 12) injection and animals administered i.c.v.-SYN (n = 12) was compared to that of heterozygous mice (n = 35) and SMNΔ7 mice (n = 22) from birth to 20 days of age. Animals were laid on their back and the time needed to flip over was measured. Three trials per day were performed for each animal.

Spontaneous Activity

The spontaneous activity of i.v.-PGK-injected (n = 11) and i.c.v.-PGK-injected (n = 13) mice was compared to that of age-matched heterozygous mice (n = 39) between 70 and 80 days of age. Distance, average speed, and rearing were assessed for 60 min using an actimeter (Bioseb) placed in a quiet room. Cage vibrations were recorded to measure locomotion, and the number of crossed infrared light beams was measured to determine rearing. Data were analyzed using Track software (Bioseb).

Motor Coordination Analysis (Rotarod)

The motor coordination of i.v.-PGK-injected (n = 17) or i.c.v.-PGK-injected (n = 12) mice was compared to that of age-matched heterozygous mice (n = 34) for 4 weeks (5 days a week) from 70 to 90 days of age using an accelerating rotarod instrument (Bioseb). The time spent on the rotarod before falling was recorded in three trials per day and per animal. The mean of the measurements from all 4 weeks was used for the analysis for each animal.

Statistical Analysis

Data are expressed as the mean ± SEM (standard error of the mean), and the differences were considered significant for $p < 0.05$. After testing for the assumption of normality, statistical significance was assessed using Student's paired t test, one-way ANOVA, or the Kruskal-Wallis test with appropriate *post hoc* tests, depending on the data and as stated in the figure legends. Survival curves were compared using the log rank Mantel-Cox test. Statistical tests were performed using Prism software (version 7.0, GraphPad).

Comparisons of the change of either body weight or the righting reflex over time were performed using a linear mixed model and the lmer function in the lme4 package. Significance for the main effects of group, time, and their interaction was then evaluated with the ANOVA function in the car package using type-II Wald chi-square tests. Tukey's *post hoc* pairwise comparisons were performed for significant group differences using the emmeans function of the emmeans package after removing the time × group interaction term. The level of statistical significance was set at $p < 0.05$ for all tests. These statistical analyses were conducted using R version 3.5.2.

SUPPLEMENTAL INFORMATION

Supplemental Information can be found online at https://doi.org/10.1016/j.ymthe.2020.05.011.

AUTHOR CONTRIBUTIONS

M.B. conceived the study. M.G.B. and A.B. planned the experiments and interpreted the results. A.B., P.S., and M.G.B. wrote the manuscript. A.B. and S.A. carried out experiments. A.B., M.R., B.G., and T.M. maintained the animals and performed the behavioral analyses and injections. A.B. and S.A. produced the AAV vectors. F.R. and P.S. scientifically contributed to the work. F.-X.L. performed the repeated-measures ANOVA.

CONFLICTS OF INTEREST

The authors declare no competing interests.

ACKNOWLEDGMENTS

The authors thank Genethon (Evry) for providing the plasmid encoding the human synapsin promoter. The authors also sincerely thank B. Cadot (Center of Research in Myology) for help in the microscopy image acquisition, M. Cohen-Tannoudji, Alexia Castiglione, and Sahar Elouej (Center of Research in Myology) for technical assistance, and D. Unni for careful proofreading. We thank S. Lefebvre for critical reading of the manuscript. This work was funded by the Association Française contre les Myopathies (AFM), the Association Institut de Myologie (AIM), the Sorbonne Université, the Institut National de la Santé et de la Recherche Médicale (INSERM), the Université Paris-Est Créteil (UPEC), and SMA Europe (Call 2012). F.R. is supported by the Association Française contre les Myopathies (AFM) via Translamuscle (project 19507).

REFERENCES

1. Pearn, J. (1978). Incidence, prevalence, and gene frequency studies of chronic childhood spinal muscular atrophy. J. Med. Genet. *15*, 409–413.
2. Prior, T.W. (2010). Perspectives and diagnostic considerations in spinal muscular atrophy. Genet. Med. *12*, 145–152.
3. Prior, T.W., Snyder, P.J., Rink, B.D., Pearl, D.K., Pyatt, R.E., Mihal, D.C., Conlan, T., Schmalz, B., Montgomery, L., Ziegler, K., et al. (2010). Newborn and carrier screening for spinal muscular atrophy. Am. J. Med. Genet. A. *152A*, 1608–1616.
4. Crawford, T.O., and Pardo, C.A. (1996). The neurobiology of childhood spinal muscular atrophy. Neurobiol. Dis. *3*, 97–110.
5. Kolb, S.J., and Kissel, J.T. (2015). Spinal muscular atrophy. Neurol. Clin. *33*, 831–846.
6. Lefebvre, S., Bürglen, L., Reboullet, S., Clermont, O., Burlet, P., Viollet, L., Benichou, B., Cruaud, C., Millasseau, P., Zeviani, M., et al. (1995). Identification and characterization of a spinal muscular atrophy-determining gene. Cell *80*, 155–165.
7. Hua, Y., Sahashi, K., Hung, G., Rigo, F., Passini, M.A., Bennett, C.F., and Krainer, A.R. (2010). Antisense correction of SMN2 splicing in the CNS rescues necrosis in a type III SMA mouse model. Genes Dev. *24*, 1634–1644.
8. Stein, C.A., and Castanotto, D. (2017). FDA-approved oligonucleotide therapies in 2017. Mol. Ther. *25*, 1069–1075.
9. Hoy, S.M. (2019). Onasemnogene abeparvovec: first global approval. Drugs *79*, 1255–1262.
10. Mendell, J.R., Al-Zaidy, S., Shell, R., Arnold, W.D., Rodino-Klapac, L.R., Prior, T.W., Lowes, L., Alfano, L., Berry, K., Church, K., et al. (2017). Single-dose gene-replacement therapy for spinal muscular atrophy. N. Engl. J. Med. *377*, 1713–1722.
11. Barkats, M. (2009). Widespread gene delivery to motor neurons using peripheral injection of AAV vectors, https://patentscope.wipo.int/search/en/detail.jsf?docId=WO2009043936&tab=PCTBIBLIO&maxRec=1000.
12. Duque, S., Joussemet, B., Riviere, C., Marais, T., Dubreil, L., Douar, A.-M., Fyfe, J., Moullier, P., Colle, M.A., and Barkats, M. (2009). Intravenous administration of self-complementary AAV9 enables transgene delivery to adult motor neurons. Mol. Ther. *17*, 1187–1196.
13. Foust, K.D., Nurre, E., Montgomery, C.L., Hernandez, A., Chan, C.M., and Kaspar, B.K. (2009). Intravascular AAV9 preferentially targets neonatal neurons and adult astrocytes. Nat. Biotechnol. *27*, 59–65.
14. Dominguez, E., Marais, T., Chatauret, N., Benkhelifa-Ziyyat, S., Duque, S., Ravassard, P., Carcenac, R., Astord, S., Pereira de Moura, A., Voit, T., and Barkats, M. (2011). Intravenous scAAV9 delivery of a codon-optimized SMN1 sequence rescues SMA mice. Hum. Mol. Genet. *20*, 681–693.
15. Le, T.T., Pham, L.T., Butchbach, M.E.R., Zhang, H.L., Monani, U.R., Coovert, D.D., Gavrilina, T.O., Xing, L., Bassell, G.J., and Burghes, A.H. (2005). SMNΔ7, the major product of the centromeric survival motor neuron (*SMN2*) gene, extends survival in mice with spinal muscular atrophy and associates with full-length SMN. Hum. Mol. Genet. *14*, 845–857.
16. Foust, K.D., Wang, X., McGovern, V.L., Braun, L., Bevan, A.K., Haidet, A.M., Le, T.T., Morales, P.R., Rich, M.M., Burghes, A.H., and Kaspar, B.K. (2010). Rescue of the spinal muscular atrophy phenotype in a mouse model by early postnatal delivery of SMN. Nat. Biotechnol. *28*, 271–274.
17. Valori, C.F., Ning, K., Wyles, M., Mead, R.J., Grierson, A.J., Shaw, P.J., and Azzouz, M. (2010). Systemic delivery of scAAV9 expressing SMN prolongs survival in a model of spinal muscular atrophy. Sci. Transl. Med. *2*, 35ra42.
18. Hinderer, C., Katz, N., Buza, E.L., Dyer, C., Goode, T., Bell, P., Richman, L.K., and Wilson, J.M. (2018). Severe toxicity in nonhuman primates and piglets following high-dose intravenous administration of an adeno-associated virus vector expressing human SMN. Hum. Gene Ther. *29*, 285–298.
19. Benkhelifa-Ziyyat, S., Besse, A., Roda, M., Duque, S., Astord, S., Carcenac, R., Marais, T., and Barkats, M. (2013). Intramuscular scAAV9-SMN injection mediates widespread gene delivery to the spinal cord and decreases disease severity in SMA mice. Mol. Ther. *21*, 282–290.
20. Armbruster, N., Lattanzi, A., Jeavons, M., Van Wittenberghe, L., Gjata, B., Marais, T., Martin, S., Vignaud, A., Voit, T., Mavilio, F., et al. (2016). Efficacy and biodistribution analysis of intracerebroventricular administration of an optimized scAAV9-SMN1 vector in a mouse model of spinal muscular atrophy. Mol. Ther. Methods Clin. Dev. *3*, 16060.
21. Glascock, J.J., Shababi, M., Wetz, M.J., Krogman, M.M., and Lorson, C.L. (2012). Direct central nervous system delivery provides enhanced protection following vector mediated gene replacement in a severe model of spinal muscular atrophy. Biochem. Biophys. Res. Commun. *417*, 376–381.
22. Meyer, K., Ferraiuolo, L., Schmelzer, L., Braun, L., McGovern, V., Likhite, S., Michels, O., Govoni, A., Fitzgerald, J., Morales, P., et al. (2015). Improving single injection CSF delivery of AAV9-mediated gene therapy for SMA: a dose-response study in mice and nonhuman primates. Mol. Ther. *23*, 477–487.
23. Passini, M.A., Bu, J., Richards, A.M., Treleaven, C.M., Sullivan, J.A., O'Riordan, C.R., Scaria, A., Kells, A.P., Samaranch, L., San Sebastian, W., et al. (2014). Translational fidelity of intrathecal delivery of self-complementary AAV9-survival motor neuron 1 for spinal muscular atrophy. Hum. Gene Ther. *25*, 619–630.
24. Robbins, K.L., Glascock, J.J., Osman, E.Y., Miller, M.R., and Lorson, C.L. (2014). Defining the therapeutic window in a severe animal model of spinal muscular atrophy. Hum. Mol. Genet. *23*, 4559–4568.
25. Bevan, A.K., Duque, S., Foust, K.D., Morales, P.R., Braun, L., Schmelzer, L., Chan, C.M., McCrate, M., Chicoine, L.G., Coley, B.D., et al. (2011). Systemic gene delivery in large species for targeting spinal cord, brain, and peripheral tissues for pediatric disorders. Mol. Ther. *19*, 1971–1980.
26. Federici, T., Taub, J.S., Baum, G.R., Gray, S.J., Grieger, J.C., Matthews, K.A., Handy, C.R., Passini, M.A., Samulski, R.J., and Boulis, N.M. (2012). Robust spinal motor neuron transduction following intrathecal delivery of AAV9 in pigs. Gene Ther. *19*, 852–859.
27. Gray, S.J., Nagabhushan Kalburgi, S., McCown, T.J., and Jude Samulski, R. (2013). Global CNS gene delivery and evasion of anti-AAV-neutralizing antibodies by intrathecal AAV administration in non-human primates. Gene Ther. *20*, 450–459.
28. Hinderer, C., Bell, P., Katz, N., Vite, C.H., Louboutin, J.-P., Bote, E., Yu, H., Zhu, Y., Casal, M.L., Bagel, J., et al. (2018). Evaluation of intrathecal routes of administration for adeno-associated viral vectors in large animals. Hum. Gene Ther. *29*, 15–24.
29. Samaranch, L., Salegio, E.A., San Sebastian, W., Kells, A.P., Foust, K.D., Bringas, J.R., Lamarre, C., Forsayeth, J., Kaspar, B.K., and Bankiewicz, K.S. (2012). Adeno-associated virus serotype 9 transduction in the central nervous system of nonhuman primates. Hum. Gene Ther. *23*, 382–389.
30. Hamilton, G., and Gillingwater, T.H. (2013). Spinal muscular atrophy: going beyond the motor neuron. Trends Mol. Med. *19*, 40–50.
31. Nash, L.A., Burns, J.K., Chardon, J.W., Kothary, R., and Parks, R.J. (2016). Spinal muscular atrophy: more than a disease of motor neurons? Curr. Mol. Med. *16*, 779–792.
32. Shababi, M., Lorson, C.L., and Rudnik-Schöneborn, S.S. (2014). Spinal muscular atrophy: a motor neuron disorder or a multi-organ disease? J. Anat. *224*, 15–28.

33. Kim, J.-K., Jha, N.N., Feng, Z., Faleiro, M.R., Chiriboga, C.A., Wei-Lapierre, L., Dirksen, R.T., Ko, C.P., and Monani, U.R. (2020). Muscle-specific *SMN* reduction reveals motor neuron-independent disease in spinal muscular atrophy models. J. Clin. Invest. *130*, 1271–1287.

34. Martínez-Hernández, R., Soler-Botija, C., Also, E., Alias, L., Caselles, L., Gich, I., Bernal, S., and Tizzano, E.F. (2009). The developmental pattern of myotubes in spinal muscular atrophy indicates prenatal delay of muscle maturation. J. Neuropathol. Exp. Neurol. *68*, 474–481.

35. Mutsaers, C.A., Wishart, T.M., Lamont, D.J., Riessland, M., Schreml, J., Comley, L.H., Murray, L.M., Parson, S.H., Lochmüller, H., Wirth, B., et al. (2011). Reversible molecular pathology of skeletal muscle in spinal muscular atrophy. Hum. Mol. Genet. *20*, 4334–4344.

36. Cifuentes-Diaz, C., Frugier, T., Tiziano, F.D., Lacène, E., Roblot, N., Joshi, V., Moreau, M.H., and Melki, J. (2001). Deletion of murine *SMN* exon 7 directed to skeletal muscle leads to severe muscular dystrophy. J. Cell Biol. *152*, 1107–1114.

37. Kariya, S., Park, G.-H., Maeno-Hikichi, Y., Leykekhman, O., Lutz, C., Arkovitz, M.S., Landmesser, L.T., and Monani, U.R. (2008). Reduced SMN protein impairs maturation of the neuromuscular junctions in mouse models of spinal muscular atrophy. Hum. Mol. Genet. *17*, 2552–2569.

38. Ling, K.K.Y., Gibbs, R.M., Feng, Z., and Ko, C.-P. (2012). Severe neuromuscular denervation of clinically relevant muscles in a mouse model of spinal muscular atrophy. Hum. Mol. Genet. *21*, 185–195.

39. Murray, L.M., Comley, L.H., Thomson, D., Parkinson, N., Talbot, K., and Gillingwater, T.H. (2008). Selective vulnerability of motor neurons and dissociation of pre- and post-synaptic pathology at the neuromuscular junction in mouse models of spinal muscular atrophy. Hum. Mol. Genet. *17*, 949–962.

40. Crawford, T.O., Sladky, J.T., Hurko, O., Besner-Johnston, A., and Kelley, R.I. (1999). Abnormal fatty acid metabolism in childhood spinal muscular atrophy. Ann. Neurol. *45*, 337–343.

41. Hua, Y., Sahashi, K., Rigo, F., Hung, G., Horev, G., Bennett, C.F., et al. (2011). Peripheral SMN restoration is essential for long-term rescue of a severe spinal muscular atrophy mouse model. Nature *478*, 123–126.

42. Vitte, J.M., Davoult, B., Roblot, N., Mayer, M., Joshi, V., Courageot, S., Tronche, F., Vadrot, J., Moreau, M.H., Kemeny, F., and Melki, J. (2004). Deletion of murine *Smn* exon 7 directed to liver leads to severe defect of liver development associated with iron overload. Am. J. Pathol. *165*, 1731–1741.

43. Bevan, A.K., Hutchinson, K.R., Foust, K.D., Braun, L., McGovern, V.L., Schmelzer, L., Ward, J.G., Petruska, J.C., Lucchesi, P.A., Burghes, A.H., and Kaspar, B.K. (2010). Early heart failure in the SMNΔ7 model of spinal muscular atrophy and correction by postnatal scAAV9-SMN delivery. Hum. Mol. Genet. *19*, 3895–3905.

44. Heier, C.R., Satta, R., Lutz, C., and DiDonato, C.J. (2010). Arrhythmia and cardiac defects are a feature of spinal muscular atrophy model mice. Hum. Mol. Genet. *19*, 3906–3918.

45. Shababi, M., Habibi, J., Yang, H.T., Vale, S.M., Sewell, W.A., and Lorson, C.L. (2010). Cardiac defects contribute to the pathology of spinal muscular atrophy models. Hum. Mol. Genet. *19*, 4059–4071.

46. Bowerman, M., Swoboda, K.J., Michalski, J.-P., Wang, G.-S., Reeks, C., Beauvais, A., Murphy, K., Woulfe, J., Screaton, R.A., Scott, F.W., and Kothary, R. (2012). Glucose metabolism and pancreatic defects in spinal muscular atrophy. Ann. Neurol. *72*, 256–268.

47. Bowerman, M., Michalski, J.-P., Beauvais, A., Murray, L.M., DeRepentigny, Y., and Kothary, R. (2014). Defects in pancreatic development and glucose metabolism in SMN-depleted mice independent of canonical spinal muscular atrophy neuromuscular pathology. Hum. Mol. Genet. *23*, 3432–3444.

48. Somers, E., Lees, R.D., Hoban, K., Sleigh, J.N., Zhou, H., Muntoni, F., Talbot, K., Gillingwater, T.H., and Parson, S.H. (2016). Vascular defects and spinal cord hypoxia in spinal muscular atrophy. Ann. Neurol. *79*, 217–230.

49. Deguise, M.-O., De Repentigny, Y., McFall, E., Auclair, N., Sad, S., and Kothary, R. (2017). Immune dysregulation may contribute to disease pathogenesis in spinal muscular atrophy mice. Hum. Mol. Genet. *26*, 801–819.

50. Hensel, N., Kubinski, S., and Claus, P. (2020). The need for SMN-independent treatments of spinal muscular atrophy (SMA) to complement SMN-enhancing drugs. Front. Neurol. *11*, 45.

51. Kügler, S., Kilic, E., and Bähr, M. (2003). Human synapsin 1 gene promoter confers highly neuron-specific long-term transgene expression from an adenoviral vector in the adult rat brain depending on the transduced area. Gene Ther. *10*, 337–347.

52. Lukashchuk, V., Lewis, K.E., Coldicott, I., Grierson, A.J., and Azzouz, M. (2016). AAV9-mediated central nervous system-targeted gene delivery via cisterna magna route in mice. Mol. Ther. Methods Clin. Dev. *3*, 15055.

53. McLean, J.R., Smith, G.A., Rocha, E.M., Hayes, M.A., Beagan, J.A., Hallett, P.J., and Isacson, O. (2014). Widespread neuron-specific transgene expression in brain and spinal cord following synapsin promoter-driven AAV9 neonatal intracerebroventricular injection. Neurosci. Lett. *576*, 73–78.

54. Ramos, D.M., d'Ydewalle, C., Gabbeta, V., Dakka, A., Klein, S.K., Norris, D.A., Matson, J., Taylor, S.J., Zaworski, P.G., Prior, T.W., et al. (2019). Age-dependent SMN expression in disease-relevant tissue and implications for SMA treatment. J. Clin. Invest. *129*, 4817–4831.

55. Nathwani, A.C., Reiss, U.M., Tuddenham, E.G.D., Rosales, C., Chowdary, P., McIntosh, J., Della Peruta, M., Lheriteau, E., Patel, N., Raj, D., et al. (2014). Long-term safety and efficacy of factor IX gene therapy in hemophilia B. N. Engl. J. Med. *371*, 1994–2004.

56. Rivera, V.M., Gao, G.P., Grant, R.L., Schnell, M.A., Zoltick, P.W., Rozamus, L.W., Clackson, T., and Wilson, J.M. (2005). Long-term pharmacologically regulated expression of erythropoietin in primates following AAV-mediated gene transfer. Blood *105*, 1424–1430.

57. Sehara, Y., Fujimoto, K.I., Ikeguchi, K., Katakai, Y., Ono, F., Takino, N., Ito, M., Ozawa, K., and Muramatsu, S.I. (2017). Persistent expression of dopamine-synthesizing enzymes 15 years after gene transfer in a primate model of Parkinson's disease. Hum. Gene Ther. Clin. Dev. *28*, 74–79.

58. Finkel, R.S., Chiriboga, C.A., Vajsar, J., Day, J.W., Montes, J., De Vivo, D.C., Yamashita, M., Rigo, F., Hung, G., Schneider, E., et al. (2016). Treatment of infantile-onset spinal muscular atrophy with nusinersen: a phase 2, open-label, dose-escalation study. Lancet *388*, 3017–3026.

59. Finkel, R.S., Mercuri, E., Darras, B.T., Connolly, A.M., Kuntz, N.L., Kirschner, J., Chiriboga, C.A., Saito, K., Servais, L., Tizzano, E., et al.; ENDEAR Study Group (2017). Nusinersen versus sham control in infantile-onset spinal muscular atrophy. N. Engl. J. Med. *377*, 1723–1732.

60. Gavrilina, T.O., McGovern, V.L., Workman, E., Crawford, T.O., Gogliotti, R.G., DiDonato, C.J., Monani, U.R., Morris, G.E., and Burghes, A.H. (2008). Neuronal SMN expression corrects spinal muscular atrophy in severe SMA mice while muscle-specific SMN expression has no phenotypic effect. Hum. Mol. Genet. *17*, 1063–1075.

61. Wang, J., Xu, G., Slunt, H.H., Gonzales, V., Coonfield, M., Fromholt, D., Copeland, N.G., Jenkins, N.A., and Borchelt, D.R. (2005). Coincident thresholds of mutant protein for paralytic disease and protein aggregation caused by restrictively expressed superoxide dismutase cDNA. Neurobiol. Dis. *20*, 943–952.

62. Park, G.-H., Maeno-Hikichi, Y., Awano, T., Landmesser, L.T., and Monani, U.R. (2010). Reduced survival of motor neuron (SMN) protein in motor neuronal progenitors functions cell autonomously to cause spinal muscular atrophy in model mice expressing the human centromeric (*SMN2*) gene. J. Neurosci. *30*, 12005–12019.

63. Jackson, K.L., Dayton, R.D., Deverman, B.E., and Klein, R.L. (2016). Better targeting, better efficiency for wide-scale neuronal transduction with the synapsin promoter and AAV-PHP.B. Front. Mol. Neurosci. *9*, 116.

64. Husain, T., Passini, M.A., Parente, M.K., Fraser, N.W., and Wolfe, J.H. (2009). Long-term AAV vector gene and protein expression in mouse brain from a small pan-cellular promoter is similar to neural cell promoters. Gene Ther. *16*, 927–932.

65. Rindt, H., Feng, Z., Mazzasette, C., Glascock, J.J., Valdivia, D., Pyles, N., Crawford, T.O., Swoboda, K.J., Patitucci, T.N., Ebert, A.D., et al. (2015). Astrocytes influence the severity of spinal muscular atrophy. Hum. Mol. Genet. *24*, 4094–4102.

66. Fallini, C., Bassell, G.J., and Rossoll, W. (2012). Spinal muscular atrophy: the role of SMN in axonal mRNA regulation. Brain Res. *1462*, 81–92.

67. Groen, E.J.N., Perenthaler, E., Courtney, N.L., Jordan, C.Y., Shorrock, H.K., van der Hoorn, D., Huang, Y.T., Murray, L.M., Viero, G., and Gillingwater, T.H. (2018).

Temporal and tissue-specific variability of SMN protein levels in mouse models of spinal muscular atrophy. Hum. Mol. Genet. *27*, 2851–2862.

68. Sleigh, J.N., Gillingwater, T.H., and Talbot, K. (2011). The contribution of mouse models to understanding the pathogenesis of spinal muscular atrophy. Dis. Model. Mech. *4*, 457–467.

69. Engle, S.J., Blaha, L., and Kleiman, R.J. (2018). Best practices for translational disease modeling using human iPSC-derived neurons. Neuron *100*, 783–797.

70. McCarty, D.M., Monahan, P.E., and Samulski, R.J. (2001). Self-complementary recombinant adeno-associated virus (scAAV) vectors promote efficient transduction independently of DNA synthesis. Gene Ther. *8*, 1248–1254.

71. Biferi, M.G., Cohen-Tannoudji, M., Cappelletto, A., Giroux, B., Roda, M., Astord, S., Marais, T., Bos, C., Voit, T., Ferry, A., and Barkats, M. (2017). A new AAV10-U7-mediated gene therapy prolongs survival and restores function in an ALS mouse model. Mol. Ther. *25*, 2038–2052.